Applied Mathematical Modelling 35 (2011) 5245–5264

Contents lists available at ScienceDirect

Applied Mathematical Modelling

journal homepage: www.elsevier.com/locate/apm

Chaos generalized synchronization of new Mathieu–Van der Pol systems with new Duffing–Van der Pol systems as functional system by GYC partial region stability theory

Zheng-Ming Ge *, Shih-Yu Li [1]

Department of Mechanical Engineering, National Chiao Tung University, 1001 Ta Hsueh Road, Hsinchu 300, Taiwan, People's Republic of China

ARTICLE INFO

Article history:
Received 30 August 2010
Received in revised form 25 February 2011
Accepted 8 March 2011
Available online 15 March 2011

Keywords:
Generalized synchronization
Chaos
Synchronization
Partial region stability theory
New Mathieu–van der Pol system
New Duffing–van der Pol system

ABSTRACT

In this paper, a new strategy by using GYC partial region stability theory is proposed to achieve generalized chaos synchronization. via using the GYC partial region stability theory, the new Lyapunov function used is a simple linear homogeneous function of states and the lower order controllers are much more simple and introduce less simulation error. Numerical simulations are given for new Mathieu–Van der Pol system and new Duffing–Van der Pol system to show the effectiveness of this strategy.

1. Introduction

In the last few years, synchronization in chaotic dynamical systems has received a great deal of interest among scientists from various fields [1–8]. The phenomenon of synchronization of two chaotic systems is fundamental in science and has a wealth of applications in technology. In recent years, more and more applications of chaos synchronization were proposed. There are many control techniques to synchronize chaotic systems, such as linear error feedback control, adaptive control, active control [9–19].

In this paper, a new chaos generalized synchronization strategy by GYC partial region stability theory is proposed [20,21]. It means that there exists a given functional relationship between the states of the master and that of the slave. via using the GYC partial region stability theory, the new Lyapunov function is a simple linear homogeneous function of states and the lower order controllers are much more simple and introduce less simulation error.

The layout of the rest of the paper is as follows. In Section 2, generalized chaos synchronization strategy by GYC partial region stability theory is proposed. In Section 3, new Mathieu–Van der pol system and new Duffing–Van der pol system are introduced. In Section 4, six simulation examples are given. In Section 5, conclusions are given.

* Corresponding author. Address: Department of Mechanical Engineering, National Chiao Tung University, 1001 Ta Hsueh Road, Hsinchu 300, Taiwan, People's Republic of China. Tel.: +886 3 5712121 55119; fax: +886 3 5720634.
E-mail address: zmg@cc.nctu.edu.tw (Z.-M. Ge).
[1] Tel.: +886 3 5712121 55179.

0307-904X/$ - see front matter © 2011 Elsevier Inc. All rights reserved.
doi:10.1016/j.apm.2011.03.022

2. Generalized Chaos Synchronization Strategy by GYC Partial Region Stability Theory

2.1. GYC Partial Region Stability Theory

Consider the differential equations of disturbed motion of a nonautonomous system in the normal form

$$\frac{dx_s}{dt} = X_s(t, x_1, \ldots, x_n), \quad (s = 1, \ldots, n), \tag{1}$$

where the function X_s is defined on the intersection of the partial region Ω (shown in Fig. 1) and

$$\sum_s x_s^2 \leqslant H \tag{2}$$

and $t > t_0$, where t_0 and H are certain positive constants. X_s which vanishes when the variables x_s are all zero, is a real valued function of $t, x_1, \ldots, x_n$. It is assumed that X_s is smooth enough to ensure the existence, uniqueness of the solution of the initial value problem. When X_s does not contain t explicitly, the system is autonomous.

Obviously, $x_s = 0$ $(s = 1, \ldots n)$ is a solution of Eq. (1). We are interested to the asymptotical stability of this zero solution on partial region Ω (including the boundary) of the neighborhood of the origin which in general may consist of several subregions (Fig.1).

Definition 1. For any given number $\varepsilon > 0$, if there exists a $\delta > 0$, such that on the closed given partial region Ω when

$$\sum_s x_{s0}^2 \leqslant \delta, \quad (s = 1, \ldots, n) \tag{3}$$

for all $t \geqslant t_0$, the inequality

$$\sum_s x_s^2 < \varepsilon, \quad (s = 1, \ldots, n) \tag{4}$$

is satisfied for the solutions of Eq. (19) on Ω, then the disturbed motion $x_s = 0$ $(s = 1, \ldots n)$ is stable on the partial region Ω.

Definition 2. If the undisturbed motion is stable on the partial region Ω, and there exists a $\delta' > 0$, so that on the given partial region Ω when

$$\sum_s x_{s0}^2 \leqslant \delta', \quad (s = 1, \ldots, n). \tag{5}$$

The equality

$$\lim_{t \to \infty} \left(\sum_s x_s^2 \right) = 0 \tag{6}$$

is satisfied for the solutions of Eq. (1) on Ω, then the undisturbed motion $x_s = 0$ $(s = 1, \ldots n)$ is asymptotically stable on the partial region Ω.

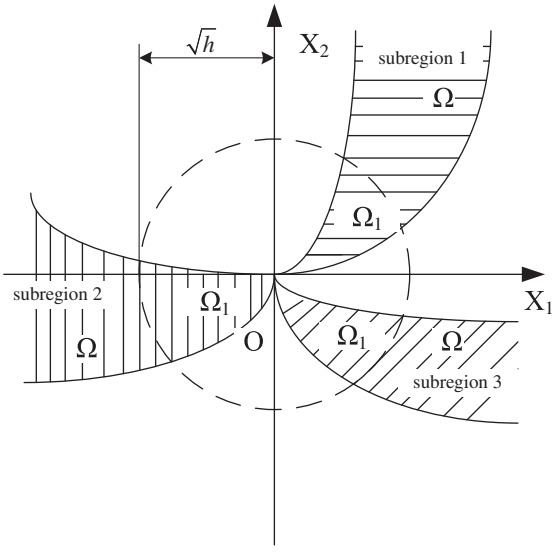

Fig. 1. Partial regions Ω and Ω_1.

The intersection of Ω and region defined by Eq. (2) is called the region of attraction.

Definition of Functions $V(t,x_1,\ldots,x_n)$: Let us consider the functions $V(t,x_1,\ldots,x_n)$ given on the intersection Ω_1 of the partial region Ω and the region

$$\sum_s x_s^2 \leqslant h, \quad (s = 1,\ldots,n) \tag{7}$$

for $t \geqslant t_0 > 0$, where t_0 and h are positive constants. We suppose that the functions are single-valued and have continuous partial derivatives and become zero when $x_1 = \cdots = x_n = 0$.

Definition 3. If there exists $t_0 > 0$ and a sufficiently small $h > 0$, so that on partial region Ω_1 and $t \geqslant t_0$, $V \geqslant 0$ (or $\leqslant 0$), then V is a positive (or negative) semidefinite, in general semidefinite, function on the Ω_1 and $t \geqslant t_0$.

Definition 4. If there exists a positive (negative) definitive function $W(x_1 \cdots x_n)$ on Ω_1, so that on the partial region Ω_1 and $t \geqslant t_0$

$$V - W \geqslant 0 (or - V - W \geqslant 0), \tag{8}$$

then $V(t,x_1,\ldots,x_n)$ is a positive definite function on the partial region Ω_1 and $t \geqslant t_0$. Eq. (1)

Definition 5. If $V(t,x_1,\ldots,x_n)$ is neither definite nor semidefinite on Ω_1 and $t \geqslant t_0$, then $V(t,x_1,\ldots,x_n)$ is an indefinite function on partial region Ω_1 and $t \geqslant t_0$. That is, for any small $h > 0$ and any large $t_0 > 0$, $V(t,x_1,\ldots,x_n)$ can take either positive or negative value on the partial region Ω_1 and $t \geqslant t_0$.

Definition 6. Bounded function *V*If there exist $t_0 > 0$, $h > 0$, so that on the partial region Ω_1, we have

$$|V(t,x_1,\ldots,x_n)| < L,$$

where L is a positive constant, then V is said to be bounded on Ω_1.

Definition 7. Function with infinitesimal upper bound If V is bounded, and for any $\lambda > 0$, there exists $\mu > 0$, so that on Ω_1 when $\sum_s x_s^2 \leqslant \mu$, and $t \geqslant t_0$, we have

$$|V(t,x_1,\ldots,x_n)| \leqslant \lambda$$

then V admits an infinitesimal upper bound on Ω_1.

Theorem 1. *If there can be found a definite function $V(t,x_1,\ldots,x_n)$ on the partial region for Eq. (1), and the derivative with respect to time based on these equations:*

$$\frac{dV}{dt} = \frac{\partial V}{\partial t} + \sum_{s=1}^{n} \frac{\partial V}{\partial x_s} X_s \tag{9}$$

is a semidefinite function on the paritial region whose sense is opposite to that of V, or if it becomes zero identically, then the undisturbed motion is stable on the partial region.

Proof. Let us assume for the sake of definiteness that V is a positive definite function. Consequently, there exists a sufficiently large number t_0 and a sufficiently small number h< H, such that on the intersection Ω_1 of partial region Ω and

$$\sum_s x_s^2 \leqslant h, \quad (s = 1,\ldots,n)$$

and $t \geqslant t_0$, the following inequality is satisfied

$$V(t,x_1,\ldots,x_n) \geqslant W(x_1,\ldots,x_n),$$

where W is a certain positive definite function which does not depend on t. Besides that, Eq. (9) may assume only negative or zero value in this region.

Let ε be an arbitrarily small positive number. We shall suppose that in any case $\varepsilon < h$. Let us consider the aggregation of all possible values of the quantities $x_1,\ldots,x_n$, which are on the intersection ω_2 of Ω_1 and

$$\sum_s x_s^2 = \varepsilon, \tag{10}$$

and let us designate by $l > 0$ the precise lower limit of the function W under this condition. By virtue of Eq. (5), we shall have

$$V(t,x_1,\ldots,x_n) \geqslant l \quad \text{for } (x_1,\ldots,x_n) \text{ on } \omega_2. \tag{11}$$

We shall now consider the quantities x_s as functions of time which satisfy the differential equations of disturbed motion. We shall assume that the initial values x_{s0} of these functions for $t = t_0$ lie on the intersection Ω_2 of Ω_1 and the region

$$\sum_s x_s^2 \leqslant \delta, \tag{12}$$

where δ is so small that

$$V(t_0, x_{10}, \ldots, x_{n0}) < l. \tag{13}$$

By virtue of the fact that $V(t_0, 0, \ldots, 0) = 0$, such a selection of the number δ is obviously possible. We shall suppose that in any case the number δ is smaller than ε.Then the inequality

$$\sum_s x_s^2 < \varepsilon, \tag{14}$$

being satisfied at the initial instant will be satisfied, in the very least, for a sufficiently small $t - t_0$, since the functions $x_s(t)$ very continuously with time. We shall show that these inequalities will be satisfied for all values $t > t_0$. Indeed, if these inequalities were not satisfied at some time, there would have to exist such an instant $t = T$ for which this inequality would become an equality. In other words, we would have

$$\sum_s x_s^2(T) = \varepsilon,$$

and consequently, on the basis of Eq. (11)

$$V(T, x_1(T), \ldots, x_n(T)) \geqslant l. \tag{15}$$

On the other hand, since $\varepsilon < h$, the inequality (Eq. (4)) is satisfied in the entire interval of time $[t_0, T]$, and consequently, in this entire time interval $\frac{dV}{dt} \leqslant 0$. This yields

$$V(T, x_1(T), \ldots, x_n(T)) \leqslant V(t_0, x_{10}, \ldots, x_{n0}),$$

which contradicts Eq. (14) on the basis of Eq. (13). Thus, the inequality (Eq. (1)) must be satisfied for all values of $t > t_0$, hence follows that the motion is stable.

Finally, we must point out that from the view-point of mathematics, the stability on partial region in general does not be related logically to the stability on whole region. If an undisturbed solution is stable on a partial region, it may be either stable or unstable on the whole region and vice versa. In specific practical problems, we do not study the solution starting within Ω_2 and running out of Ω. □

Theorem 2. *If in satisfying the conditions of theorem 1, the derivative $\frac{dV}{dt}$ is a definite function on the partial region with opposite sign to that of V and the function V itself permits an infinitesimal upper limit, then the undisturbed motion is asymptotically stable on the partial region.*

Proof. Let us suppose that V is a positive definite function on the partial region and that consequently, $\frac{dV}{dt}$ is negative definite. Thus on the intersection Ω_1 of Ω and the region defined by Eq. (4) and $t \geqslant t_0$ there will be satisfied not only the inequality (Eq. (5)), but the following inequality as will:

$$\frac{dV}{dt} \leqslant -W_1(x_1, \ldots x_n), \tag{16}$$

where W_1 is a positive definite function on the partial region independent of t. Let us consider the quantities x_s as functions of time which satisfy the differential equations of disturbed motion assuming that the initial values $x_{s0} = x_s(t_0)$ of these quantities satisfy the inequalities (Eq. (12)). Since the undisturbed motion is stable in any case, the magnitude δ may be selected so small that for all values of $t \geqslant t_0$ the quantities x_s remain within Ω_1. Then, on the basis of Eq. (16) the derivative of function $V(t, x_1(t), \ldots, x_n(t))$ will be negative at all times and, consequently, this function will approach a certain limit, as t increases without limit, remaining larger than this limit at all times. We shall show that this limit is equal to some positive quantity different from zero. Then for all values of $t \geqslant t_0$ the following inequality will be satisfied:

$$V(t, x_1(t), \ldots, x_n(t)) > \alpha, \tag{17}$$

where $\alpha > 0$.

Since V permits an infinitesimal upper limit, it follows from this inequality that

$$\sum_s x_s^2(t) \geqslant \lambda, \quad (s = 1, \ldots, n), \tag{18}$$

where λ is a certain sufficiently small positive number. Indeed, if such a number λ did not exist, that is, if the quantity $\sum_s x_s(t)$ were smaller than any preassigned number no matter how small, then the magnitude $V(t, x_1(t), \ldots, x_n(t))$, as follows from the definition of an infinitesimal upper limit, would also be arbitrarily small, which contradicts (17).

If for all values of $t \geqslant t_0$ the inequality (Eq. (18)) is satisfied, then Eq. (16) shows that the following inequality will be satisfied at all times:

$$\frac{dV}{dt} \leqslant -l_1,$$

where l_1 is positive number different from zero which constitutes the precise lower limit of the function $W_1(t,x_1(t),\ldots,x_n(t))$ under condition (Eq. (18)). Consequently, for all values of $t \geqslant t_0$ we shall have:

$$V(t,x_1(t),\ldots,x_n(t)) = V(t_0,x_{10},\ldots,x_{n0}) + \int_{t_0}^{t} \frac{dV}{dt}dt \leqslant V(t_0,x_{10},\ldots,x_{n0}) - l_1(t-t_0),$$

which is, obviously, in contradiction with Eq. (17). The contradiction thus obtained shows that the function $V(t,x_1(t),\ldots,x_n(t))$ approached zero as t increase without limit. Consequently, the same will be true for the function $W(x_1(t),\ldots,x_n(t))$ as well, from which it follows directly that

$$\lim_{t\to\infty} x_s(t) = 0, \quad (s = 1,\ldots,n),$$

which proves the theorem. □

2.2. Generalized Chaos Synchronization Strategy

Consider the following unidirectional coupled chaotic systems

$$\begin{aligned} \dot{\mathbf{x}} &= \mathbf{f}(t,\mathbf{x}) \\ \dot{\mathbf{y}} &= \mathbf{h}(t,\mathbf{y}) + \mathbf{u}, \end{aligned} \tag{19}$$

Where $\mathbf{x} = [x_1,x_2,\ldots,x_n]^T \in R^n$, $\mathbf{y} = [y_1,y_2,\ldots,y_n]^T \in R^n$ denote the master state vector and slave state vector respectively, $\mathbf{f}$ and $\mathbf{h}$ are nonlinear vector functions, and $\mathbf{u} = [u_1,u_2,\ldots,u_n]^T \in R^n$ is a control input vector.

The generalized synchronization can be accomplished when $t \to \infty$, the limit of the error vector $\mathbf{e} = [e_1,e_{2,\ldots},e_n]^T$ approaches zero:

$$\lim_{t\to\infty} \mathbf{e} = 0, \tag{20}$$

where

$$\mathbf{e} = \mathbf{G}(\mathbf{x}) - \mathbf{y}. \tag{21}$$

$G(x)$ is a given function of x.

By using the partial region stability theory, the Lyapunov function is easier to find, since the linear terms of the entries of $\mathbf{e}$ can be used to construct the definite Lyapunov function and the controllers can be designed in lower order.

3. New Chaotic Mathieu–Van der Pol System and New Chaotic Duffing–Van der Pol System

This section introduces new Mathieu–van der Pol system and new Duffing–van der Pol system, respectively.

3.1. New Mathieug–van der Pol system

Mathieu equation and van der Pol equation are two typical nonlinear non-autonomous systems:

$$\begin{cases} \dot{x}_1 = x_2 \\ \dot{x}_2 = -(a + b\sin\omega t)x_1 - (a + b\sin\omega t)x_1^3 - cx_2 + d\sin\omega t \end{cases} \tag{22}$$

$$\begin{cases} \dot{x}_3 = x_4 \\ \dot{x}_4 = -ex_3 + f(1 - x_3^2)x_4 + g\sin\omega t. \end{cases} \tag{23}$$

Exchanging sinωt in Eq. (22) with x_3 and sinωt in Eq. (23) with x_1, we obtain the autonomous new Mathieu–van der Pol system:

$$\begin{cases} \dot{x}_1 = x_2 \\ \dot{x}_2 = -(a + bx_3)x_1 - (a + bx_3)x_1^3 - cx_2 + dx_3 \\ \dot{x}_3 = x_4 \\ \dot{x}_4 = -ex_3 + f(1 - x_3^2)x_4 + gx_1, \end{cases} \tag{24}$$

where a, b, c, d, e, f, g are uncertain parameter. This system exhibits chaos when the parameters of system are $a = 10$, $b = 3$, $c = 0.4$, $d = 70$, $e = 1$, $f = 5$, $g = 0.1$ and the initial states of system are $(x_{10},x_{20},x_{30},x_{40})$=(0.1,-0.5, 0.1,-0.5), its phase portraits and Lyapunov exponent as shown in Figs. 2 and 3.

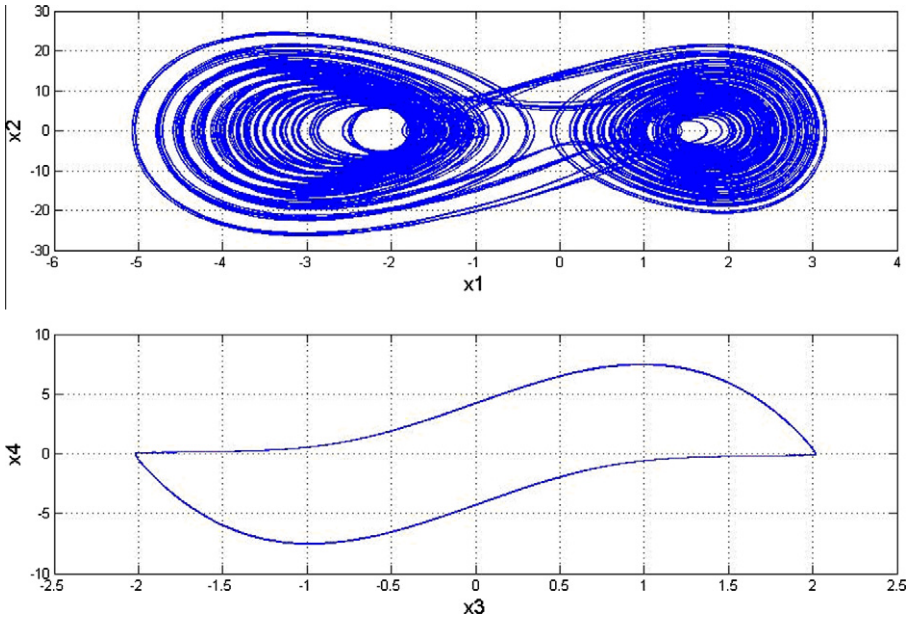

Fig. 2. Phase portraits of new chaotic Mathieu–Van der Pol System.

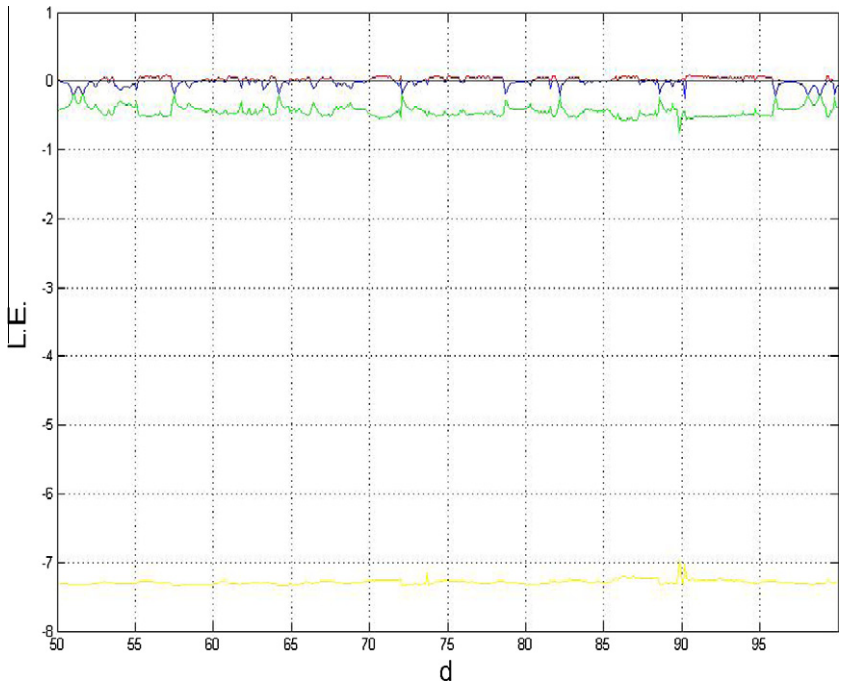

Fig. 3. Lyapunov exponents of new chaotic Mathieu–Van der Pol System.

3.2. New Duffing–van der Pol system

Duffing equation and van der Pol equation are two typical nonlinear non-autonomous systems:

$$\begin{cases} \dot{z}_1 = z_2 \\ \dot{z}_2 = -z_1 - z_1^3 - hz_2 + i\sin\omega t \end{cases} \tag{25}$$

$$\begin{cases} \dot{z}_3 = z_4 \\ \dot{z}_4 = -jz_3 + k(1 - z_3^2)z_4 + l\sin\omega t. \end{cases} \tag{26}$$

Exchanging sinωt in Eq. (25) with z_3 and sinωt in Eq. (26) with z_1, we obtain the autonomous master new Duffing–van der Pol system:

$$\begin{cases} \dot{z}_1 = z_2 \\ \dot{z}_2 = -z_1 - z_1^3 - hz_2 + iz_3 \\ \dot{z}_3 = z_4 \\ \dot{z}_4 = -jz_3 + k(1 - z_3^2)z_4 + lz_1, \end{cases} \tag{27}$$

where h, i, j, k, l are uncertain parameter. This system exhibits chaos when the parameters of system are $h = 0.0006$, $j = 1$, $k = 5$, $i = 0.67$ and $l = 0.05$ and initial states is $(2, 2.4, 5, 6)$, its phase portraits and Lyapunov exponents as shown in Figs. 4 and 5.

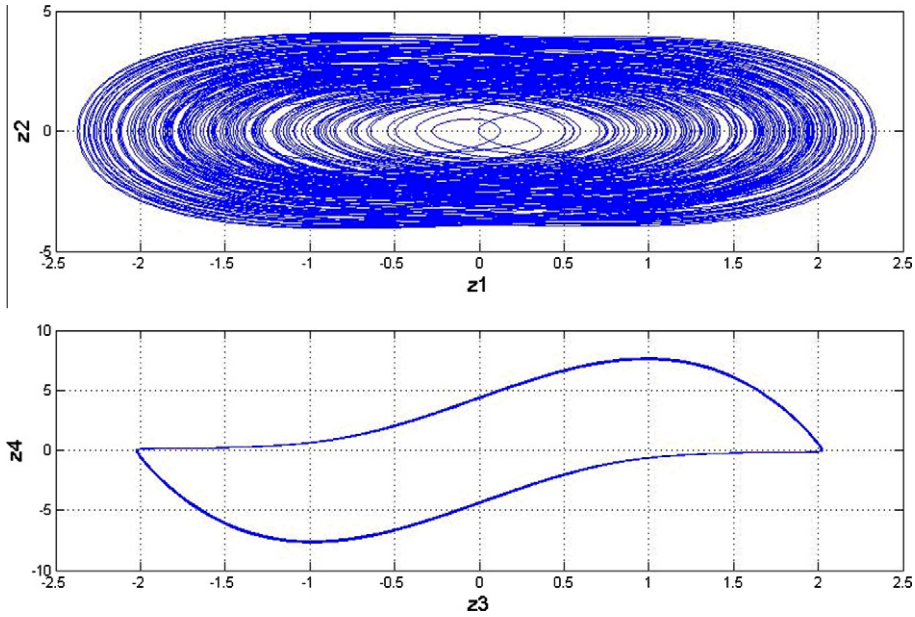

Fig. 4. Phase portraits of new chaotic Duffing–Van der Pol System.

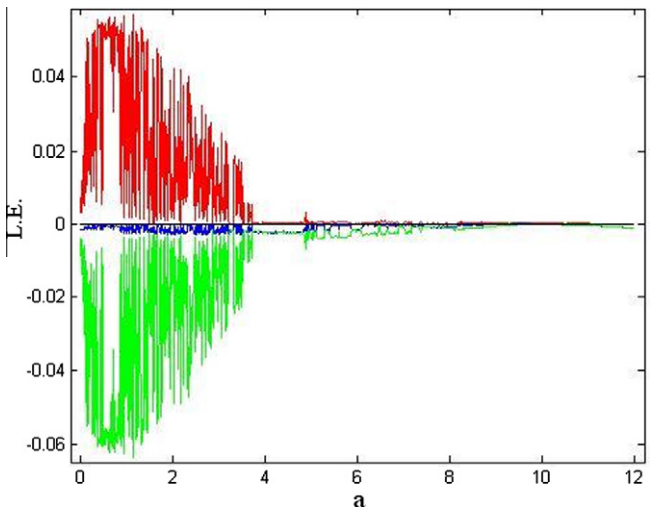

Fig. 5. Lyapunov exponents of new chaotic Duffing-Van der Pol System.

4. Numerical simulations

The two unidirectional coupled new chaotic Mathieu–Van der pol systems are shown as follows:

$$\begin{aligned}
\dot{x}_1 &= x_2 \\
\dot{x}_2 &= -(a+bx_3)x_1 - (a+bx_3)x_1^3 - cx_2 + dx_3 \\
\dot{x}_3 &= x_4 \\
\dot{x}_4 &= -ex_3 + f\left(1-x_3^2\right)x_4 + gx_1,
\end{aligned} \tag{28}$$

$$\begin{aligned}
\dot{y}_1 &= y_2 + u_1 \\
\dot{y}_2 &= -(a+by_3)y_1 - (a+by_3)y_1^3 - cy_2 + dy_3 + u_2 \\
\dot{y}_3 &= y_4 + u_3 \\
\dot{y}_4 &= -ey_3 + f\left(1-y_3^2\right)y_4 + gy_1 + u_4.
\end{aligned}$$

CASE I. The generalized synchronization error function is $e_i = (x_i - y_i + 100)$, $(i = 1,2,3,4.)$.
The addition of 100 makes the error dynamics always happens in first quadrant. Our goal is$y_i = x_i + 100$, i.e.

$$\lim_{t\to\infty} e_i = \lim_{t\to\infty}(x_i - y_i + 100) = 0 \quad (i = 1,2,3,4). \tag{29}$$

The error dynamics becomes:

$$\begin{aligned}
\dot{e}_1 &= \dot{x}_1 - \dot{y}_1 = x_2 - y_2 - u_1, \\
\dot{e}_2 &= \dot{x}_2 - \dot{y}_2 = -((a+bx_3)x_1 - (a+by_3)y_1) - \left((a+bx_3)x_1^3 - (a+by_3)y_1^3\right) - c(x_2 - y_2) + d(x_3 - y_3) - u_2, \\
\dot{e}_3 &= \dot{x}_3 - \dot{y}_3 = x_4 - y_4 - u_3, \\
\dot{e}_4 &= \dot{x}_4 - \dot{y}_4 = -e(x_3 - y_3) + f\left(\left(1-x_3^2\right)x_4 - \left(1-y_3^2\right)y_4\right) + g(x_1 - y_1) - u_4.
\end{aligned} \tag{30}$$

System parameters are chosen as $a = 10$, $b = 3$, $c = 0.4$, $d = 70$,$e = 1$, $f = 5$, $g = 0.1$ and initial states are $(x_{10},x_{20},x_{30},x_{40})$=(0.1, − 0.5,0.1, − 0.5), $(y_{10},y_{20},y_{30},y_{40})$=(0.3, − 0.1,0.3, − 0.1). Before control action, the error dynamics always happens in first quadrant as shown in Fig. 6. By GYC partial region stability, one can choose a Lyapunov function in the form of a positive definite function in first quadrant:

$$V = e_1 + e_2 + e_3 + e_4. \tag{31}$$

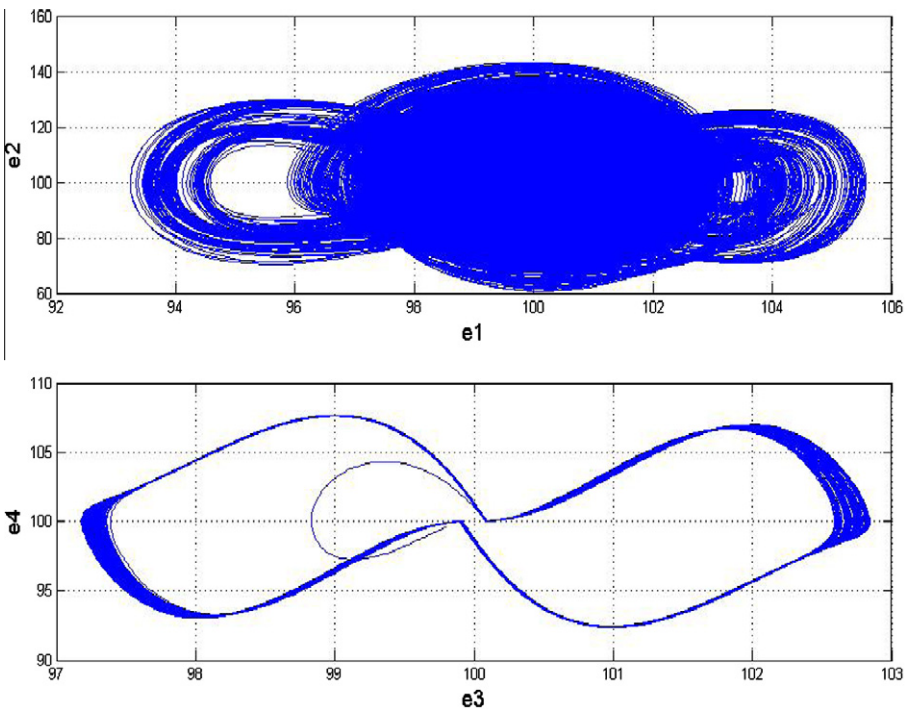

Fig. 6. Phase portraits of error dynamics for Case I.

Its time derivative through Eq. (29) is

$$\begin{aligned}\dot{V} = \dot{e}_1 + \dot{e}_2 + \dot{e}_3 + \dot{e}_4 = (x_2 - y_2 - u_1) + (-((a + bx_3)x_1 - (a + by_3)y_1) - ((a + bx_3)x_1^3 - (a + by_3)y_1^3) - c(x_2 - y_2) \\ + d(x_3 - y_3) - u_2) + (x_4 - y_4 - u_3) + (-e(x_3 - y_3) + f((1 - x_3^2)x_4 - (1 - y_3^2)y_4) + g(x_1 - y_1) - u_4).\end{aligned} \tag{32}$$

Choose

$$\begin{aligned}u_1 &= (x_2 - y_2) + e_1, \\ u_2 &= (-((a + bx_3)x_1 - (a + by_3)y_1) - ((a + bx_3)x_1^3 - (a + by_3)y_1^3) - c(x_2 - y_2) + d(x_3 - y_3)) + e_2, \\ u_3 &= (x_4 - y_4) + e_3, \\ u_4 &= (-e(x_3 - y_3) + f((1 - x_3^2)x_4 - (1 - y_3^2)y_4) + g(x_1 - y_1)) + e_4.\end{aligned} \tag{33}$$

We obtain

$$\dot{V} = -e_1 - e_2 - e_3 - e_4 < 0, \tag{34}$$

which is negative definite function in the first quadrant. Four state errors versus time and time histories of states are shown in Figs. 7 and 8.

CASE II. The generalized synchronization error function is $e_i = (x_i - y_i + F_i \sin\omega t + 100)$, $(i=1,2,3,4)$.
The addition of 100 makes the error dynamics always happens in first quadrant.
Our goal is $y_i = x_i + F_i \sin\omega t + 100$, i.e.

$$\lim_{t\to\infty} e_i = \lim_{t\to\infty}(x_i - y_i + F_i \sin\omega t + 100) = 0 \quad (i = 1,2,3,4), \tag{35}$$

Where $F_1 = F_2 = F_3 = F_4 = F = 10$, $\omega = 0.5$.
The error dynamics becomes

$$\begin{aligned}\dot{e}_1 &= x_2 - y_2 - u_1 + F\omega\cos\omega t, \\ \dot{e}_2 &= -((a + bx_3)x_1 - (a + by_3)y_1) - ((a + bx_3)x_1^3 - (a + by_3)y_1^3) - c(x_2 - y_2) + d(x_3 - y_3) - u_2 + F\omega\cos\omega t, \\ \dot{e}_3 &= x_4 - y_4 - u_3 + F\omega\cos\omega t, \\ \dot{e}_4 &= -e(x_3 - y_3) + f((1 - x_3^2)x_4 - (1 - y_3^2)y_4) + g(x_1 - y_1) - u_4 + F\omega\cos\omega t.\end{aligned} \tag{36}$$

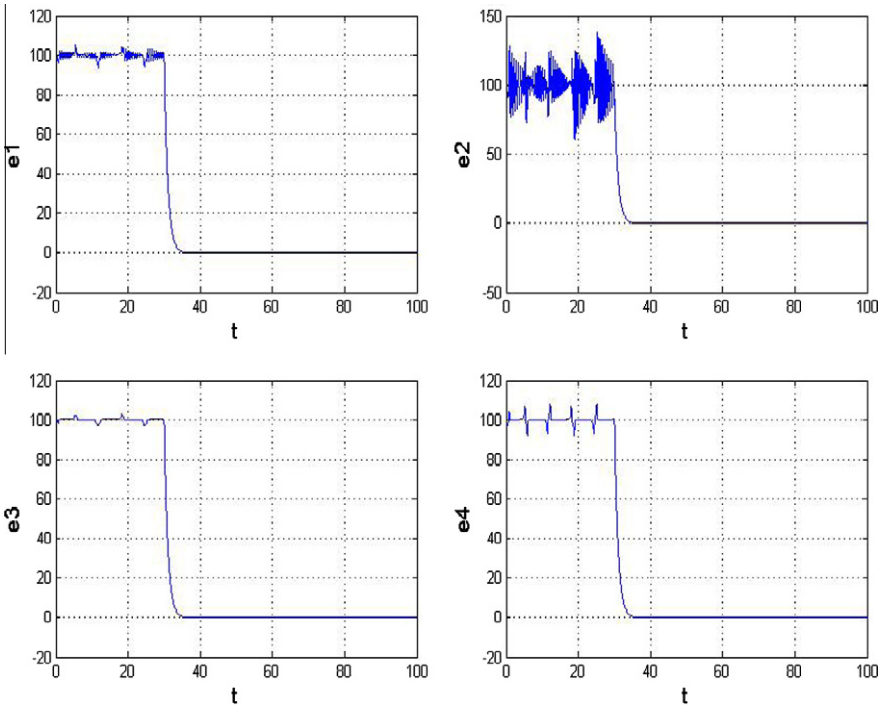

Fig. 7. Time histories of errors for Case I.

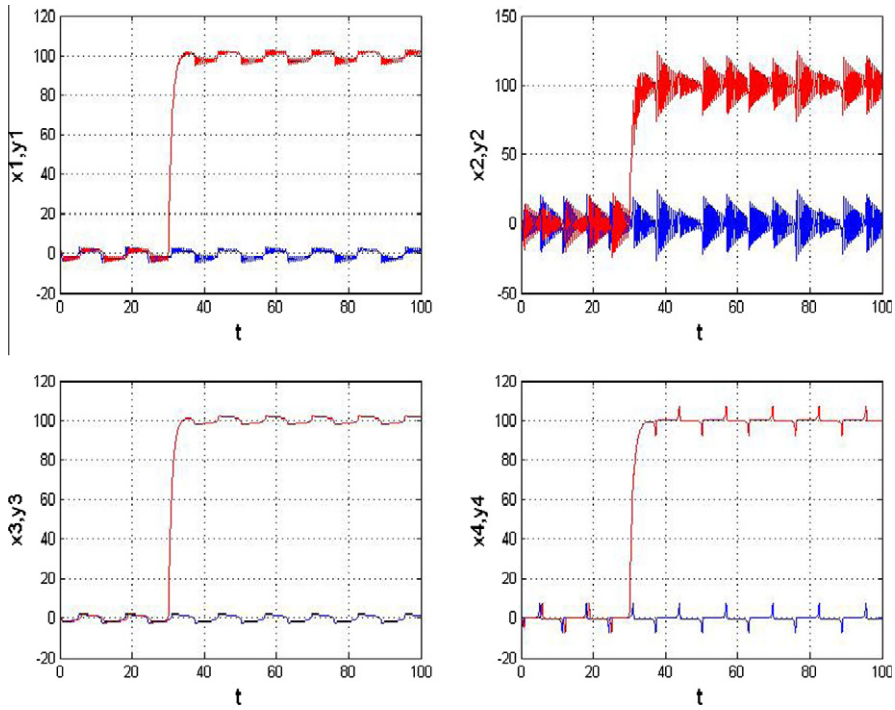

Fig. 8. Time histories of x_1, x_2, x_3, y_1, y_2, y_3 for Case I.

System parameters are chosen as $a = 10$, $b = 3$, $c = 0.4$, $d = 70$,$e = 1$, $f = 5$, $g = 0.1$ and initial states are $(x_{10},x_{20},x_{30},x_{40})$= $(0.1, -0.5, 0.1, -0.5)$, $(y_{10},y_{20},y_{30},y_{40})$=$(0.3, -0.1, 0.3, -0.1)$. Before control action, the error dynamics always happens in first quadrant as shown in Fig. 9. By GYC partial region stability, one can choose a Lyapunov function in the form of a positive definite function in first quadrant:

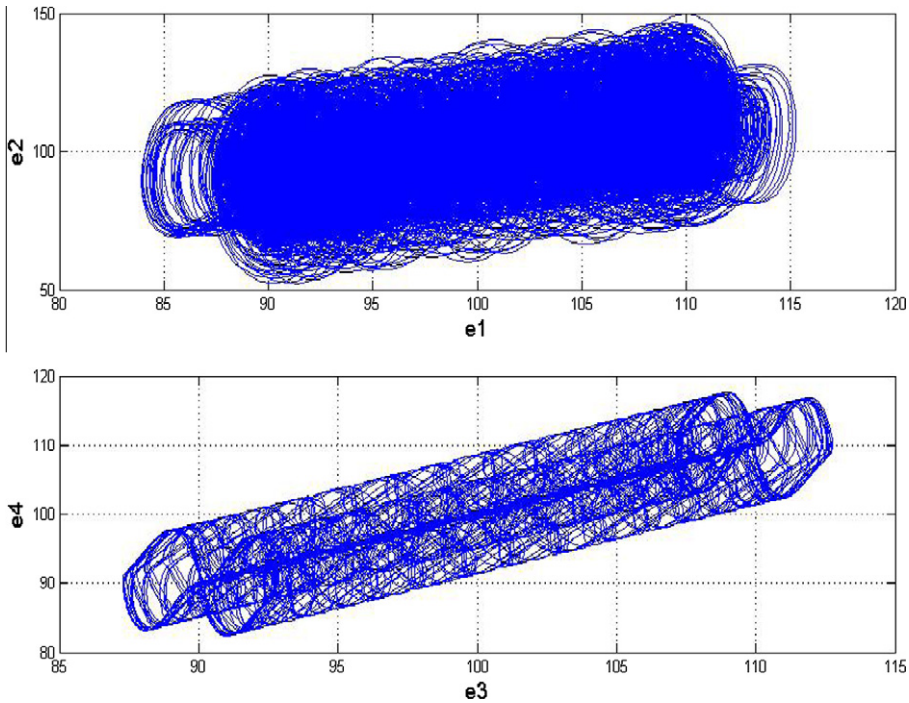

Fig. 9. Phase portraits of error dynamics for Case II.

$$V = e_1 + e_2 + e_3 + e_4. \tag{37}$$

Its time derivative through Eq. (35) is

$$\begin{aligned}\dot{V} &= \dot{e}_1 + \dot{e}_2 + \dot{e}_3 + \dot{e}_4 \\ &= (x_2 - y_2 - u_1 + F\omega\cos\omega t) + (-((a+bx_3)x_1 - (a+by_3)y_1) - ((a+bx_3)x_1^3 - (a+by_3)y_1^3) - c(x_2 - y_2) \\ &\quad + d(x_3 - y_3) - u_2 + F\omega\cos\omega t) + (x_4 - y_4 - u_3 + F\omega\cos\omega t) + (-e(x_3 - y_3) + f((1 - x_3^2)x_4 - (1 - y_3^2)y_4) \\ &\quad + g(x_1 - y_1) - u_4 + F\omega\cos\omega t).\end{aligned} \tag{38}$$

Choose

$$\begin{aligned}u_1 &= (x_2 - y_2) + F\omega\cos\omega t + e_1 \\ u_2 &= (-((a+bx_3)x_1 - (a+by_3)y_1) - ((a+bx_3)x_1^3 - (a+by_3)y_1^3) - c(x_2 - y_2) + d(x_3 - y_3)) + F\omega\cos\omega t + e_2 \\ u_3 &= (x_4 - y_4) + F\omega\cos\omega t + e_3 \\ u_4 &= (-e(x_3 - y_3) + f((1 - x_3^2)x_4 - (1 - y_3^2)y_4) + g(x_1 - y_1)) + F\omega\cos\omega t + e_4.\end{aligned} \tag{39}$$

We obtain

$$\dot{V} = -e_1 - e_2 - e_3 - e_4 < 0 \tag{40}$$

which is a negative definite function in the first quadrant. Three state errors versus time and time histories of $x_i - y_i + 100$ and $-F_i \sin wt$ are shown in Figs. 10 and 11.

CASE III. The generalized synchronization error function is $e_i = x_i - y_i + F_i e^{\sin\omega t} + 100$, ($i$=1 2, 3, 4).
The addition of 100 makes the error dynamics always happens in first quadrant.
Our goal is $y_i = x_i + F_i e^{\sin\omega t} + 100$, i.e.

$$\lim_{t\to\infty} e_i = \lim_{t\to\infty}(x_i - y_i + F_i e^{\sin\omega t} + 100) = 0 \quad (i = 1, 2, 3, 4). \tag{41}$$

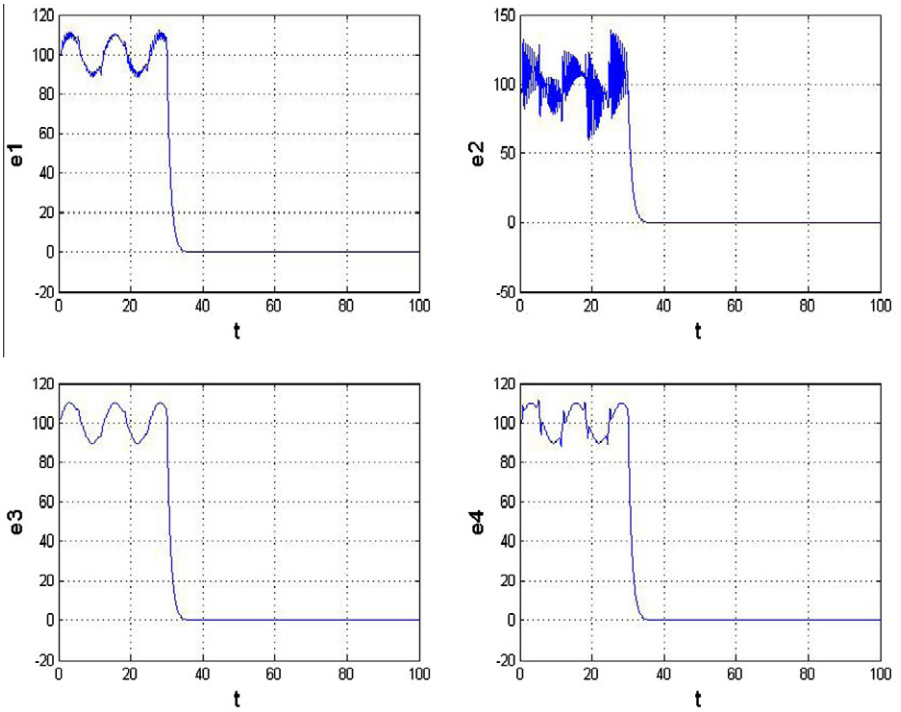

Fig. 10. Time histories of errors for Case II.

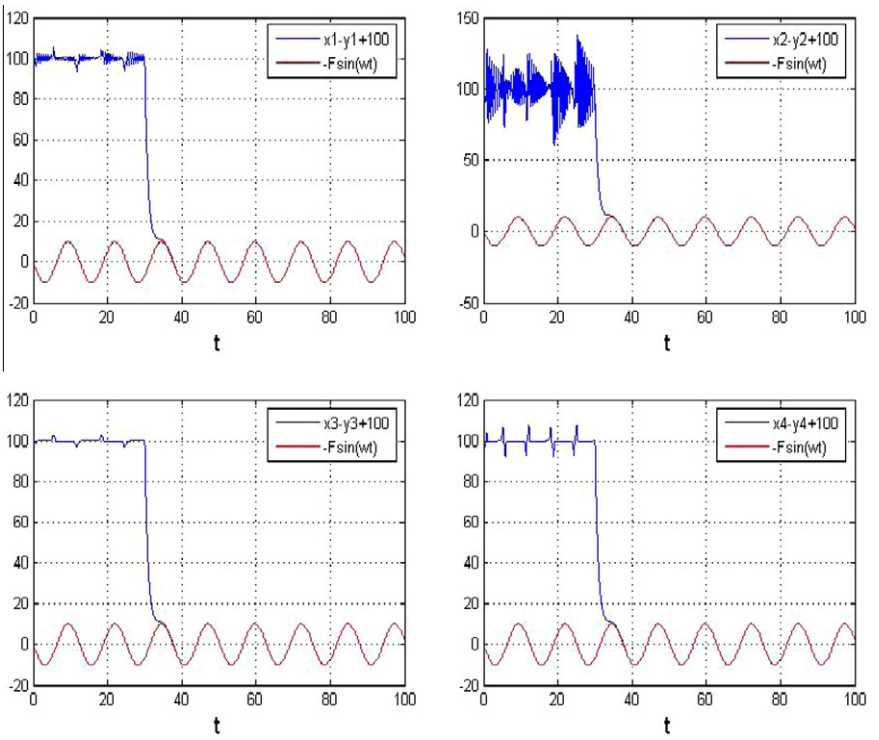

Fig. 11. Time histories of $x_i - y_i + 100$ and $-F\sin\omega t$ for Case II.

The error dynamics becomes

$$\begin{aligned}
\dot{e}_1 &= x_2 - y_2 - u_1 + F\omega e^{\sin\omega t}\cos\omega t,\\
\dot{e}_2 &= -((a+bx_3)x_1 - (a+by_3)y_1) - ((a+bx_3)x_1^3 - (a+by_3)y_1^3) - c(x_2-y_2) + d(x_3-y_3) - u_2 + F\omega e^{\sin\omega t}\cos\omega t,\\
\dot{e}_3 &= x_4 - y_4 - u_3 + F\omega e^{\sin\omega t}\cos\omega t,\\
\dot{e}_4 &= -e(x_3-y_3) + f((1-x_3^2)x_4 - (1-y_3^2)y_4) + g(x_1-y_1) - u_4 + F\omega e^{\sin\omega t}\cos\omega t.
\end{aligned} \tag{42}$$

System parameters are chosen as $a = 10$, $b = 3$, $c = 0.4$, $d = 70$, $e = 1$, $f = 5$, $g = 0.1$, $F_1 = F_2 = F_3 = F_4 = F = 10$, $\omega = 0.5$ and initial states are $(x_{10},x_{20},x_{30},x_{40})=(0.1,-0.5,0.1,-0.5)$, $(y_{10},y_{20},y_{30},y_{40})=(0.3,-0.1,0.3,-0.1)$. Before control action, the error dynamics always happens in first quadrant as shown in Fig. 12. By GYC partial region stability, one can choose a Lyapunov function in the form of a positive definite function in first quadrant:

$$V = e_1 + e_2 + e_3 + e_4. \tag{43}$$

Its time derivative through Eq. (41) is

$$\begin{aligned}
\dot{V} = \dot{e}_1 + \dot{e}_2 + \dot{e}_3 + \dot{e}_4 &= (x_2 - y_2 - u_1 + F\omega e^{\sin\omega t}\cos\omega t) + (-((a+bx_3)x_1 - (a+by_3)y_1) - ((a+bx_3)x_1^3 - (a+by_3)y_1^3)\\
&\quad - c(x_2-y_2) + d(x_3-y_3) - u_2 + F\omega e^{\sin\omega t}\cos\omega t) + (x_4 - y_4 - u_3 + F\omega e^{\sin\omega t}\cos\omega t)\\
&\quad + (-e(x_3-y_3) + f((1-x_3^2)x_4 - (1-y_3^2)y_4) + g(x_1-y_1) - u_4 + F\omega e^{\sin\omega t}\cos\omega t).
\end{aligned} \tag{44}$$

Choose

$$\begin{aligned}
u_1 &= (x_2 - y_2) + F\omega e^{\sin\omega t}\cos\omega t + e_1,\\
u_2 &= (-((a+bx_3)x_1 - (a+by_3)y_1) - ((a+bx_3)x_1^3 - (a+by_3)y_1^3) - c(x_2-y_2) + d(x_3-y_3)) + F\omega e^{\sin\omega t}\cos\omega t + e_2,\\
u_3 &= (x_4 - y_4) + F\omega e^{\sin\omega t}\cos\omega t + e_3,\\
u_4 &= (-e(x_3-y_3) + f((1-x_3^2)x_4 - (1-y_3^2)y_4) + g(x_1-y_1)) + F\omega e^{\sin\omega t}\cos\omega t + e_4.
\end{aligned} \tag{45}$$

We obtain

$$\dot{V} = -e_1 - e_2 - e_3 - e_4 < 0 \tag{46}$$

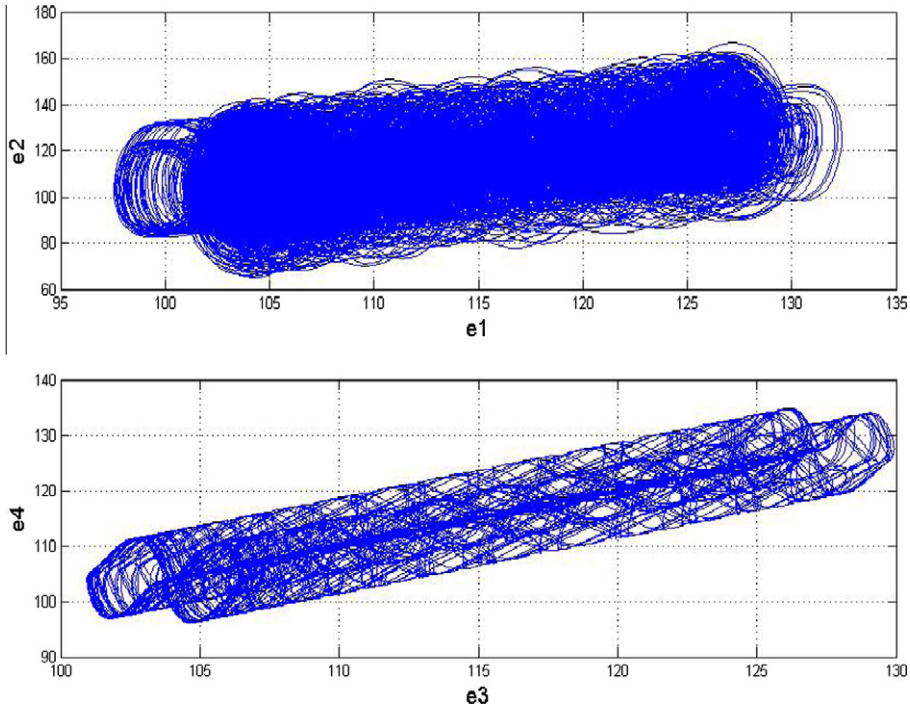

Fig. 12. Phase portraits of error dynamics for Case III.

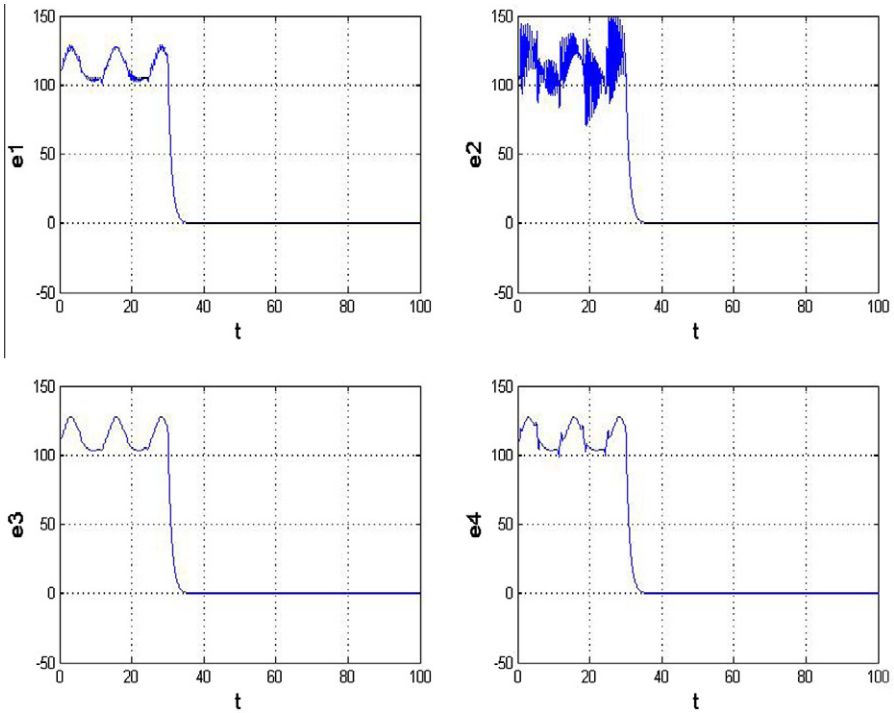

Fig. 13. Time histories of errors for Case III.

which is a negative definite function in the first quadrant. Three state errors versus time and time histories of $x_i - y_i + 100$ and $-F_i\, e^{\sin wt}$ are shown in Figs. 13 and 14.

CASE IV. The generalized synchronization error function is $e_i = \frac{1}{2}x_i^2 - y_i + 100$, ($i$=1,2,3,4). The addition of 100 makes the error dynamics always happens in first quadrant.

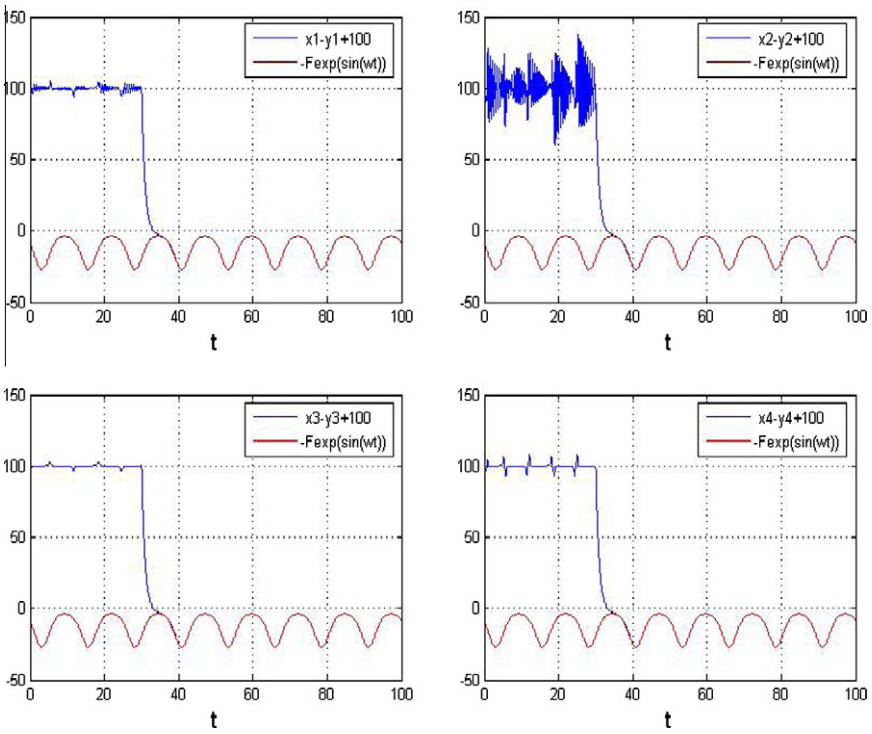

Fig. 14. Time histories of $x_i - y_i + 100$ and $-Fe^{\sin(wt)}$ for Case III.

Our goal is $y_i = \frac{1}{2}x_i^2 + 100$, i.e.

$$\lim_{t\to\infty} e_i = \lim_{t\to\infty}\left(\frac{1}{2}x_i^2 - y_i + 100\right) \quad (i = 1,2,3,4) \tag{47}$$

The error dynamics becomes

$$\begin{aligned}
\dot{e}_1 &= x_1\dot{x}_1 - \dot{y}_1 = x_1x_2 - y_2 - u_1,\\
\dot{e}_2 &= x_2\dot{x}_2 - \dot{y}_2 = -((a+bx_3)x_2x_1 - (a+by_3)y_1) - ((a+bx_3)x_2x_1^3 - (a+by_3)y_1^3) - c(x_2^2 - y_2) + d(x_2x_3 - y_3) - u_2,\\
\dot{e}_3 &= x_3\dot{x}_3 - \dot{y}_3 = x_3x_4 - y_4 - u_3,\\
\dot{e}_4 &= x_4\dot{x}_4 - \dot{y}_4 = -e(x_4x_3 - y_3) + f((1-x_3^2)x_4^2 - (1-y_3^2)y_4) + g(x_4x_1 - y_1) - u_4.
\end{aligned} \tag{48}$$

System parameters are chosen as $a = 10$, $b = 3$, $c = 0.4$, $d = 70$,$e = 1$, $f = 5$, $g = 0.1$ and initial states are $(x_{10},x_{20},x_{30},x_{40})$= $(0.1, -0.5, 0.1, -0.5)$, $(y_{10},y_{20},y_{30},y_{40})$=$(0.3, -0.1, 0.3, -0.1)$. Before control action, the error dynamics always happens in first quadrant as shown in Fig. 15. By GYC partial region stability, one can choose a Lyapunov function in the form of a positive definite function in first quadrant:

$$V = e_1 + e_2 + e_3 + e_4. \tag{49}$$

Its time derivative through Eq. (47) is

$$\begin{aligned}
\dot{V} = \dot{e}_1 + \dot{e}_2 + \dot{e}_3 + \dot{e}_4 &= (x_1x_2 - y_2 - u_1) + (-((a+bx_3)x_2x_1 - (a+by_3)y_1) - ((a+bx_3)x_2x_1^3 - (a+by_3)y_1^3) - c(x_2^2 - y_2)\\
&\quad + d(x_2x_3 - y_3) - u_2) + (x_3x_4 - y_4 - u_3) + (-e(x_4x_3 - y_3) + f((1-x_3^2)x_4^2 - (1-y_3^2)y_4) + g(x_4x_1 - y_1) - u_4).
\end{aligned} \tag{50}$$

Choose

$$\begin{aligned}
u_1 &= x_1x_2 - y_2 + e_1,\\
u_2 &= -((a+bx_3)x_2x_1 - (a+by_3)y_1) - ((a+bx_3)x_2x_1^3 - (a+by_3)y_1^3) - c(x_2^2 - y_2) + d(x_2x_3 - y_3) + e_2,\\
u_3 &= x_3x_4 - y_4 + e_3,\\
u_4 &= -e(x_4x_3 - y_3) + f((1-x_3^2)x_4^2 - (1-y_3^2)y_4) + g(x_4x_1 - y_1) + e_4.
\end{aligned} \tag{51}$$

We obtain

$$\dot{V} = -e_1 - e_2 - e_3 - e_4 < 0, \tag{52}$$

which is a negative definite function in the first quadrant. Three state errors versus time is shown in Fig. 16.

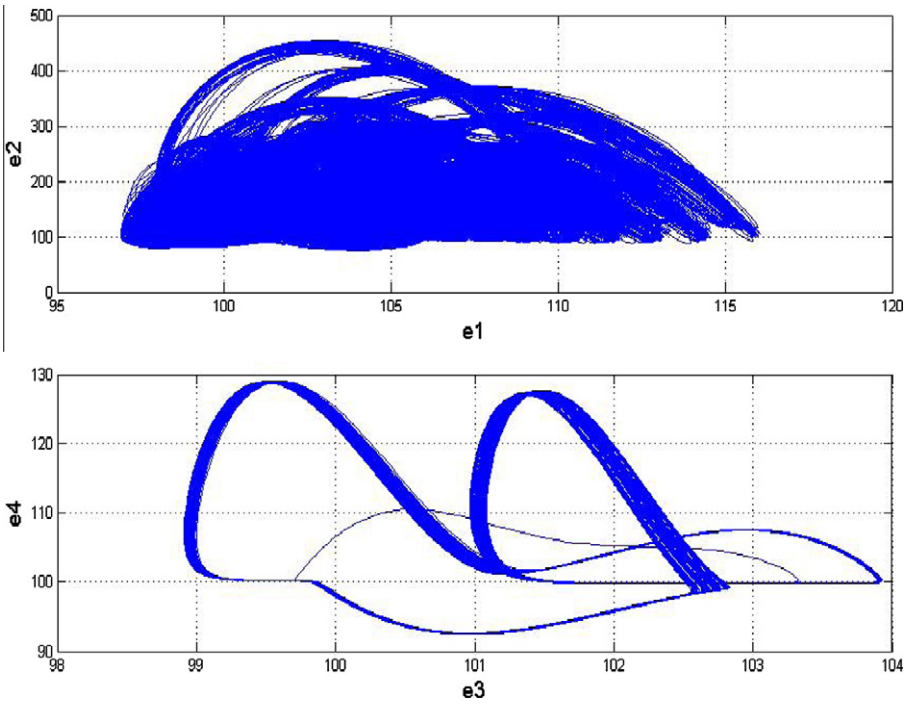

Fig. 15. Phase portraits of error dymanics for Case IV.

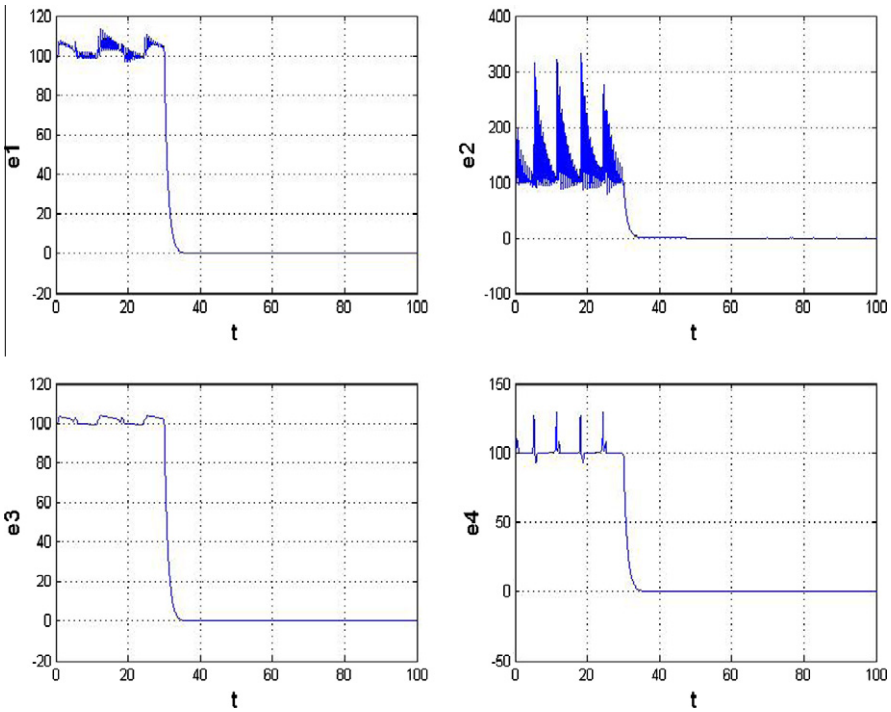

Fig. 16. Time histories of errors for Case IV.

CASE V. The generalized synchronization error function is $e_i = \frac{1}{3}x_i^3 - y_i + 10000$ (i=1,2,3,4).
The addition of 10000 makes the error dynamics always happens in first quadrant.
Our goal is $y_i = \frac{1}{3}x_i^3 + 10000$, i.e.

$$\lim_{t\to\infty} e_i = \lim_{t\to\infty}\left(\frac{1}{3}x_i^3 - y_i + 10000\right)(i = 1, 2, 3, 4). \tag{53}$$

The error dynamics becomes

$$\begin{aligned}
\dot{e}_1 &= x_1^2\dot{x}_1 - \dot{y}_1 = x_1^2x_2 - y_2 - u_1,\\
\dot{e}_2 &= x_2^2\dot{x}_2 - \dot{y}_2 = -((a+bx_3)x_2^2x_1 - (a+by_3)y_1) - ((a+bx_3)x_2^2x_1^3 - (a+by_3)y_1^3) - c(x_2^3 - y_2) + d(x_2^2x_3 - y_3) - u_2,\\
\dot{e}_3 &= x_3^2\dot{x}_3 - \dot{y}_3 = x_3^2x_4 - y_4 - u_3,\\
\dot{e}_4 &= x_4^2\dot{x}_4 - \dot{y}_4 = -e(x_4^2x_3 - y_3) + f((1-x_3^2)x_4^3 - (1-y_3^2)y_4) + g(x_4^2x_1 - y_1) - u_4.
\end{aligned} \tag{54}$$

System parameters are chosen as $a = 10$, $b = 3$, $c = 0.4$, $d = 70$,$e = 1$, $f = 5$, $g = 0.1$ and initial states are $(x_{10},x_{20},x_{30},x_{40})$= $(0.1, -0.5, 0.1, -0.5)$, $(y_{10},y_{20},y_{30},y_{40})$=$(0.3, -0.1, 0.3, -0.1)$. Before control action, the error dynamics always happens in first quadrant as shown in Fig. 17. By GYC partial region stability, one can choose a Lyapunov function in the form of a positive definite function in first quadrant:

$$V = e_1 + e_2 + e_3 + e_4. \tag{55}$$

Its time derivative through Eq. (53) is

$$\begin{aligned}
\dot{V} = \dot{e}_1 + \dot{e}_2 + \dot{e}_3 + \dot{e}_4 = (x_1^2x_2 - y_2 - u_1) + (-((a+bx_3)x_2^2x_1 - (a+by_3)y_1) - ((a+bx_3)x_2^2x_1^3 - (a+by_3)y_1^3) - c(x_2^3 - y_2)\\
+ d(x_2^2x_3 - y_3) - u_2) + (x_3^2x_4 - y_4 - u_3) + (-e(x_4^2x_3 - y_3) + f((1-x_3^2)x_4^3 - (1-y_3^2)y_4) + g(x_4^2x_1 - y_1) - u_4)).
\end{aligned} \tag{56}$$

Choose

$$\begin{aligned}
u_1 &= x_1^2x_2 - y_2 + e_1,\\
u_2 &= -((a+bx_3)x_2^2x_1 - (a+by_3)y_1) - ((a+bx_3)x_2^2x_1^3 - (a+by_3)y_1^3) - c(x_2^3 - y_2) + d(x_2^2x_3 - y_3) + e_2,\\
u_3 &= x_3^2x_4 - y_4 + e_3,\\
u_4 &= -e(x_4^2x_3 - y_3) + f((1-x_3^2)x_4^3 - (1-y_3^2)y_4) + g(x_4^2x_1 - y_1) + e_4.
\end{aligned} \tag{57}$$

We obtain

$$\dot{V} = -e_1 - e_2 - e_3 - e_4 < 0. \tag{58}$$

which is a negative definite function in the first quadrant. Three state errors versus time is shown in Fig. 18.

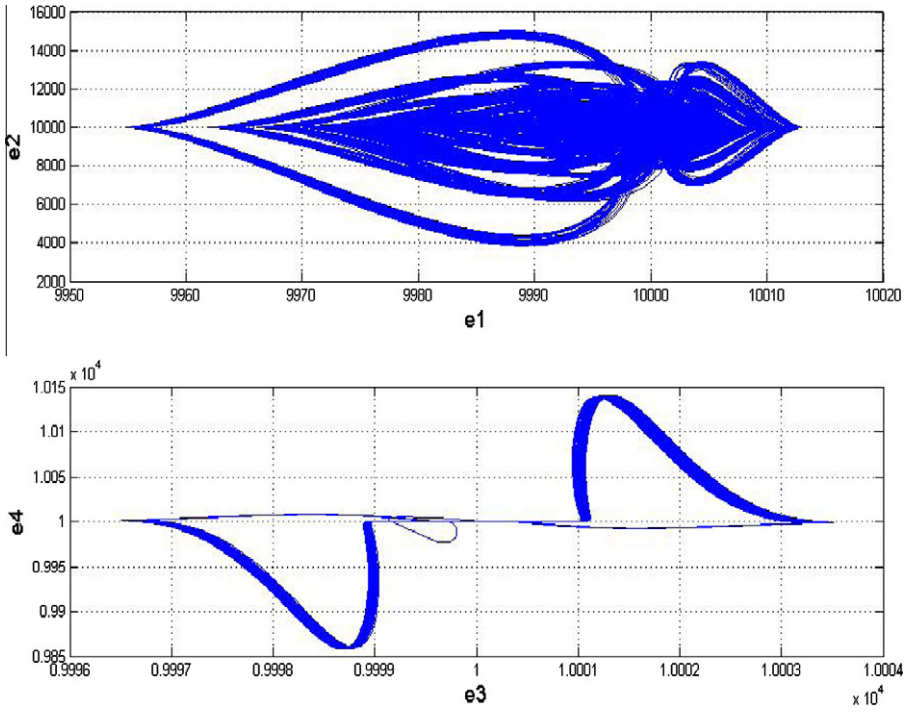

Fig. 17. Phase portraits of error dymanics for Case V.

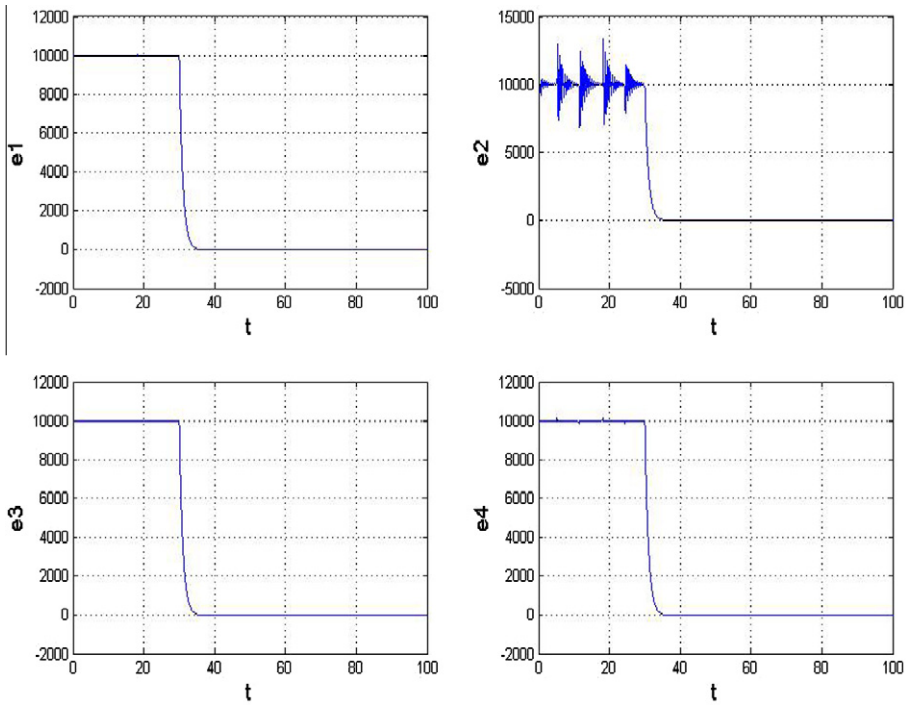

Fig. 18. Time histories of errors for Case V.

CASE VI. The generalized synchronization error function is $e_i = x_i - y_i + z_i + 100, z_i (i=1,2,3,4)$ is the states of new chaotic Duffing–Van der pol system.

The functional system for synchronization is new Duffing-Van der pol system and initial states is (2,2.4,5,6), system parameters $h = 0.0006$, $j = 1$, $k = 5$, $i = 0.67$ and $l = 0.05$.

$$\begin{aligned}
\dot{z}_1 &= z_2,\\
\dot{z}_2 &= -z_1 - z_1^3 - hz_2 + iz_3,\\
\dot{z}_3 &= z_4,\\
\dot{z}_4 &= -jz_3 + k(1 - z_3^2)z_4 + lz_1.
\end{aligned} \tag{59}$$

We have

$$\lim_{t\to\infty} e_i = \lim_{t\to\infty}(x_i - y_i + z_i + 100) = 0 (i = 1, 2, 3, 4) \tag{60}$$

The error dynamics becomes

$$\begin{aligned}
\dot{e}_1 &= \dot{x}_1 + \dot{z}_1 - \dot{y}_1 = x_2 + z_2 - y_2 - u_1,\\
\dot{e}_2 &= \dot{x}_2 + \dot{z}_2 - \dot{y}_2 = -((a + bx_3)x_1 - (a + by_3)y_1) - ((a + bx_3)x_1^3 - (a + by_3)y_1^3) - c(x_2 - y_2)\\
&\quad + d(x_3 - y_3) + (-z_1 - z_1^3 - hz_2 + iz_3) - u_2,\\
\dot{e}_3 &= \dot{x}_3 + \dot{z}_3 - \dot{y}_3 = x_4 + z_4 - y_4 - u_3,\\
\dot{e}_4 &= \dot{x}_4 + \dot{z}_4 - \dot{y}_4 = -e(x_3 - y_3) + f((1 - x_3^2)x_4 - (1 - y_3^2)y_4) + g(x_1 - y_1) - u_4 + (-jz_3 + k(1 - z_3^2)z_4 + lz_1).
\end{aligned} \tag{61}$$

System parameters are chosen as $a = 10$, $b = 3$, $c = 0.4$, $d = 70, e = 1$, $f = 5$, $g = 0.1$ and initial states are $(x_{10}, x_{20}, x_{30}, x_{40}) = (0.1, -0.5, 0.1, -0.5)$, $(y_{10}, y_{20}, y_{30}, y_{40}) = (0.3, -0.1, 0.3, -0.1)$. Before control action, the error dynamics always happens in first quadrant as shown in Fig. 19. By GYC partial region stability, one can choose a Lyapunov function in the form of a positive definite function in first quadrant:

$$V = e_1 + e_2 + e_3 + e_4. \tag{62}$$

Its time derivative through Eq. (60) is

$$\begin{aligned}
\dot{V} = \dot{e}_1 + \dot{e}_2 + \dot{e}_3 + \dot{e}_4 &= (x_2 + z_2 - y_2 - u_1) + (-((a + bx_3)x_1 - (a + by_3)y_1) - ((a + bx_3)x_1^3\\
&\quad - (a + by_3)y_1^3) - c(x_2 - y_2) + d(x_3 - y_3) + (-z_1 - z_1^3 - hz_2 + iz_3) - u_2) + (x_4 + z_4 - y_4 - u_3)\\
&\quad + (-e(x_3 - y_3) + f((1 - x_3^2)x_4 - (1 - y_3^2)y_4) + g(x_1 - y_1) - u_4 + (-jz_3 + k(1 - z_3^2)z_4 + lz_1)).
\end{aligned} \tag{63}$$

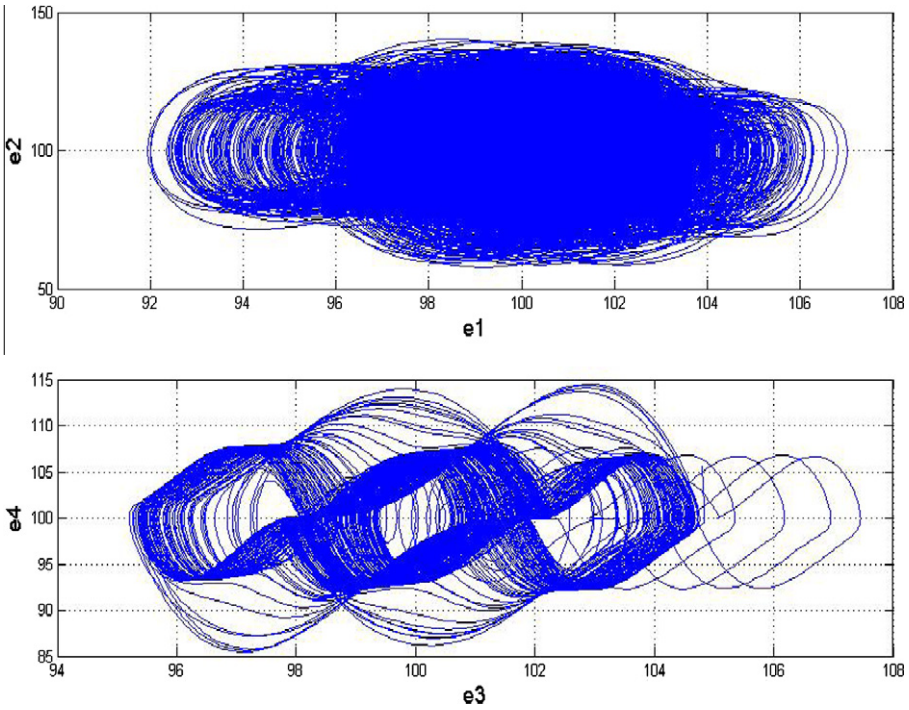

Fig. 19. Phase portraits of error dymanics for Case VI.

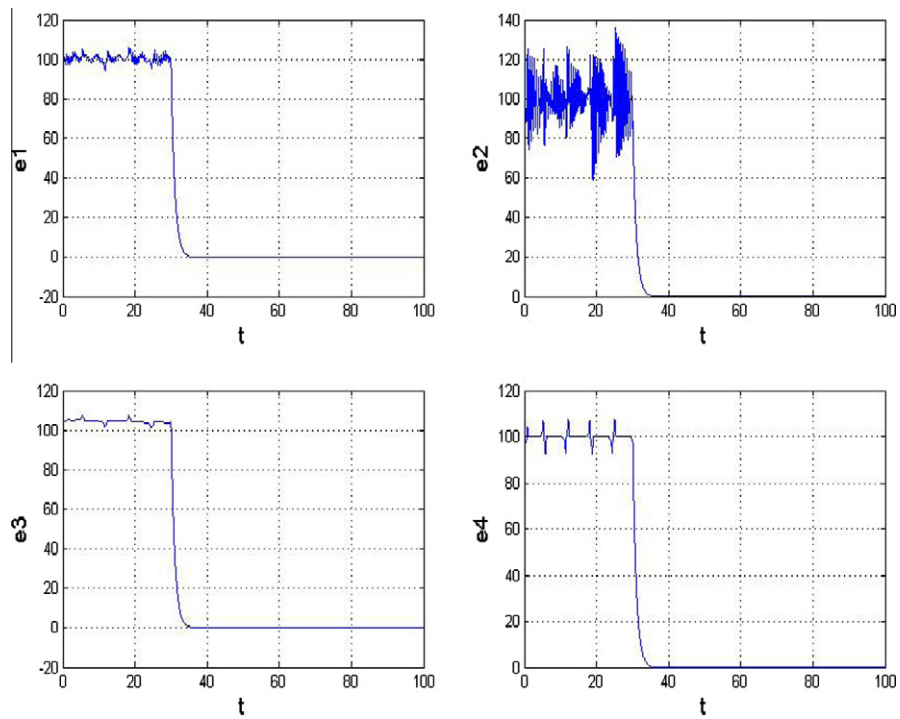

Fig. 20. Time histories of errors for Case VI.

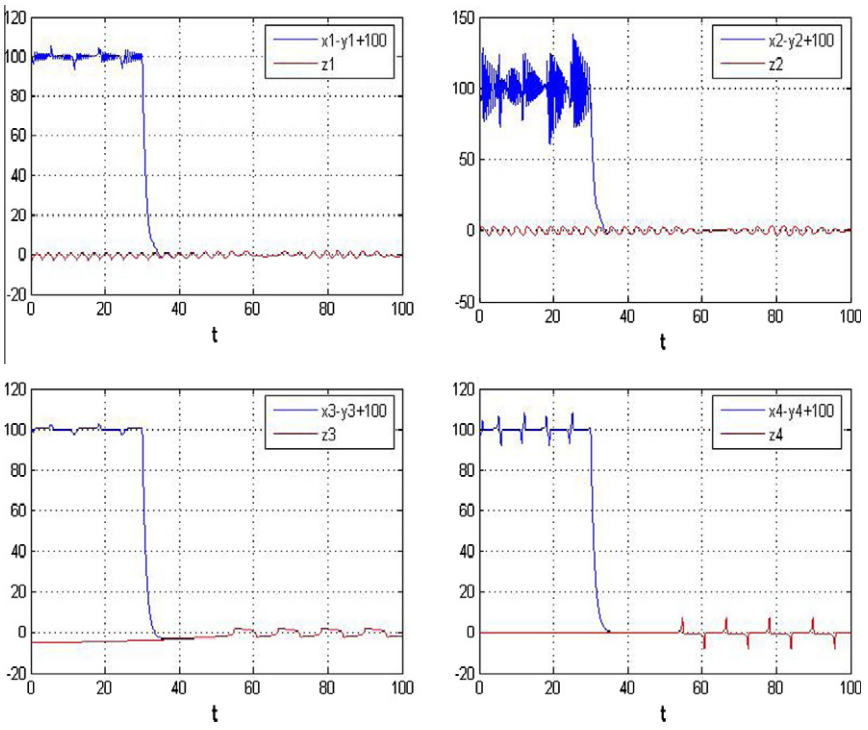

Fig. 21. Time histories of $x_i - y_i + 100$ and $-z_i$ for Case VI.

Choose

$$\begin{aligned}
u_1 &= x_2 + z_2 - y_2 + e_1,\\
u_2 &= -((a+bx_3)x_1 - (a+by_3)y_1) - ((a+bx_3)x_1^3 - (a+by_3)y_1^3) - c(x_2 - y_2) + d(x_3 - y_3) + (-z_1 - z_1^3 - hz_2 + iz_3) + e_2,\\
u_3 &= x_4 + z_4 - y_4 + e_3,\\
u_4 &= -e(x_3 - y_3) + f((1 - x_3^2)x_4 - (1 - y_3^2)y_4) + g(x_1 - y_1) + e_4 + (-jz_3 + k(1 - z_3^2)z_4 + lz_1).
\end{aligned} \tag{64}$$

We obtain

$$\dot{V} = -e_1 - e_2 - e_3 - e_4 < 0, \tag{65}$$

which is a negative definite function in the first quadrant. Four state errors versus time and time histories of $x_i - y_i + 100$ and $-z_i$ are shown in Figs. 20 and 21.

5. Conclusions

In this paper, a new strategy by using GYC partial region stability theory is proposed to achieve generalized chaos synchronization. via using the GYC partial region stability theory, the new Lyapunov function used is a simple linear homogeneous function of states and the lower order controllers are much simpler and introduce less simulation error. The new chaotic Mathieu–Van der pol system and new chaotic Duffing–Van der pol system are used as simulation examples which confirm the scheme effectively.

Acknowledgment

This research was supported by the National Science Council, Republic of China, under Grant No. NSC 96-2221-E-009-145-MY3.

References

[1] E. Ott, C. Grebogi, J.A. Yorke, Controlling chaos, Phys. Rev. Lett. 64 (1990) 1196–1199.
[2] K. Pyragas, Continuous control of chaos by self-controlling feedback, Phys. Lett. A 170 (1992) 421–428.

[3] Y. Chen, X. Wu, Z. Gui, Global synchronization criteria for a class of third-order non-autonomous chaotic systems via linear state error feedback control, Appl. Math. Model. 34 (2010) 4161–4170.
[4] R. Femat, G.S. Perales, On the chaos synchronization phenomenon, Phys. Lett. A 262 (1999) 50–60.
[5] X. Mu, L. Pei, Synchronization of the near-identical chaotic systems with the unknown parameters, Appl. Math. Model. 34 (2010) 1788–1797.
[6] J. Lu, X. Wu, J. Lu, Synchronization of a unified chaotic system and the application in secure communication, Phys. Lett. A 305 (2002) 365–370.
[7] Z.M. Ge, C.C. Chen, Phase synchronization of coupled chaotic multiple time scales systems, Chaos Solitons Fract. 20 (2004) 639–647.
[8] W. Zhang, J. Huang, P. Wei, Weak synchronization of chaotic neural networks with parameter mismatch via periodically intermittent control, Appl. Math. Model. 35 (2011) 612–620.
[9] H.K. Chen, Global chaos synchronization of new chaotic systems via nonlinear control, Chaos Solitons Fract. 23 (2005) 1245–1251.
[10] X. Yang, J. Cao, Finite-time stochastic synchronization of complex networks original research article, Appl. Math. Model. 34 (2010) 3631–3641.
[11] C.K. Weng, A. Ray, X. Dai, Modelling of power plant dynamics and uncertainties for robust control synthesis, Appl. Math. Model. 20 (1996) 501–512.
[12] J.H. Park, Adaptive synchronization of rossler system with uncertain parameters, Chaos Solitons Fract. 25 (2005) 333–338.
[13] J.H. Park, Adaptive synchronization of hyperchaotic chen system with uncertain parameters, Chaos Solitons Fract. 26 (2005) 959–964.
[14] C. Wan, J. Chang, H.T. Yau, J.L. Chen, Nonlinear dynamic analysis of a hybrid squeeze-film damper-mounted rigid rotor lubricated with couple stress fluid and active control, Appl. Math. Model. 34 (2010) 2493–2507.
[15] Y. Tang, J.A. Fang, M. Xia, X. Gu, Synchronization of Takagi–Sugeno fuzzy stochastic discrete-time complex networks with mixed time-varying delays, Appl. Math. Model. 34 (2010) 843–855.
[16] Z.M. Ge, W.Y. Leu, Anti-control of chaos of two-degrees-of- freedom louderspeaker system and chaos synchronization of different order systems, Chaos Solitons Fract. 20 (2004) 503–521.
[17] Z.M. Ge, Y.S. Chen, Synchronization of unidirectional coupled chaotic systems via partial stability, Chaos Solitons Fract. 21 (2004) 101–111.
[18] Z.M. Ge, C.M. Chang, Chaos synchronization and parameters identification of single time scale brushless dc motors, Chaos Solitons Fract. 20 (2004) 883–903.
[19] Z.M. Ge, Y.S. Chen, Synchronization of unidirectional coupled chaotic systems via partial stability, Chaos Solitons Fract. 21 (2004) 101–111.
[20] Z.M. Ge, C. W Yao, H.K. Chen, Stability on partial region in dynamics, J. Chinese Soc. Mech. Eng. 15 (2) (1994) 140–151.
[21] Z.M. Ge, H.K. Chen, Three Asymptotical Stability Theorems on Partial Region with Applications, Jpn. J. Appl. Phys. 37 (1998) 2762–2773.